Improved Structural Analysis Technique for Orthogonal Weave Carbon-Carbon Materials

GERARD C. PARDOEN*
University of California, Irvine, Calif.

An approximate technique is presented that enables one to use two-dimensional axisymmetric solid computer codes for the analysis of three-dimensional rectangularly orthotropic materials fabricated into axisymmetric shapes and loaded axisymmetrically. The technique consists of modifying the polar coordinate constitutive relations to accomodate a rectangularly orthotropic material. Specifically the proposed constitutive modification: accounts for the transverse orthotropy by including G_{xy} in the equations as an independent variable; degenerates to the transversely isotropic relations for $E_x = E_y = E$ and $G_{xy} = E_x/2(1+\nu_{xy})$; and accurately predicts the stresses in a rotating and thermally loaded rectangularly orthotropic disk whereas analyses restricted to the assumption of transverse isotropy can lead to significant errors.

Nomenclature

a	= outer radius of disk
$\mathbf{C}, \mathbf{C}^*$	= compliance, modified compliance matrices (mxm)
$\mathbf{D}_i$	= vector of element nodal displacements (nxl)
$\mathbf{E}_i, \mathbf{E}_i^*$	= element elasticity matrix, modified element elasticity matrix (mxm)
E_x, E_y	= elastic moduli in x, y directions
G_{xy}	= shear modulus in x-y plane
$\mathbf{K}_i$	= element stiffness matrix (nxn)
m	= number of stress components
n	= number of nodal displacements per element
r	= radial coordinate
$\mathbf{T}, \mathbf{T}^{-1}, \mathbf{T}^T$	= transformation matrix, its inverse and transpose (mxm)
$T(r)$	= radial temperature distribution
T_0, T_1	= arbitrary temperature values
U_i	= strain energy of ith element
α_x, α_y	= coefficients of thermal expansion in x, y directions
β	= nondimensional anisotropy parameter
$\gamma_{xy}, \gamma_{r\theta}$	= shear strain in rectangular and polar coordinates
$\boldsymbol{\varepsilon}_i$	= vector of element strains (mxl)
$\boldsymbol{\varepsilon}_{xyz}, \boldsymbol{\varepsilon}_{r\theta z}$	= vector of element strains in rectangular xyz and polar $r\theta z$ coordinates (mxl)
$\varepsilon_x, \varepsilon_y, \varepsilon_z$	= direct strain components in x, y, z directions
θ	= circumferential coordinate
ν_{ij}	= Poisson's ratio, defined as: $-$(strain in j-direction/strain in i-direction) due to $\sigma_i \neq 0$ and all other stress components $= 0$
ρ	= mass density (mass/volume)
$\boldsymbol{\sigma}_{xyz}, \boldsymbol{\sigma}_{r\theta z}$	= vector of element stresses in rectangular and polar coordinates (mxl)
$\sigma_x, \sigma_y, \sigma_z$	= direct stress components in x, y, z directions
σ_r, σ_θ	= direct stress components in polar coordinates
$\tau_{xy}, \tau_{r\theta}$	= shear stress in rectangular and polar coordinates

Introduction

THE ubiquitous solid-of-revolution stress analysis computer codes such as SAAS III[1] are usually limited to modeling material behavior as either transversely isotropic or polar orthotropic. The recent interest in three-dimensional (3D) composite materials for re-entry vehicle nosetip applications presents a significant problem in trying to use these codes since the material properties are not axisymmetric. A typical 3D composite material such as carbon-carbon consists of reinforcing fibers bundled in three orthogonal directions as shown in Fig. 1. The woven preform is then impregnated with a suitable matrix material and processed to achieve the desired properties. For analysis purposes these 3D composite materials are usually considered to be homogeneous orthotropic, it being common engineering practice to ignore the inhomogeneity or discreteness of the reinforcements. There are, of course, various techniques available for the more detailed micromechanical behavior of composites.[2] It would be desirable to use the two-dimensional axisymmetric computer codes for the analysis of 3D orthotropic materials fabricated into axisymmetric shapes and loaded axisymmetrically in Fig. 2. Unfortunately, the material properties as well as the stress and strain states are not axisymmetric thereby invalidating the fundamental assumptions of axial symmetry. Previously the only alternative was to employ either a three-dimensional finite element code[3] (usually too costly to justify) or a pseudo three-dimensional code[4] that accounts for the principal material directions. However, this paper presents an approximate technique for using axisymmetric computer codes to accurately predict the stress-strain states for at least one rz plane. Specifically a minor modification to the constitutive relations is proposed

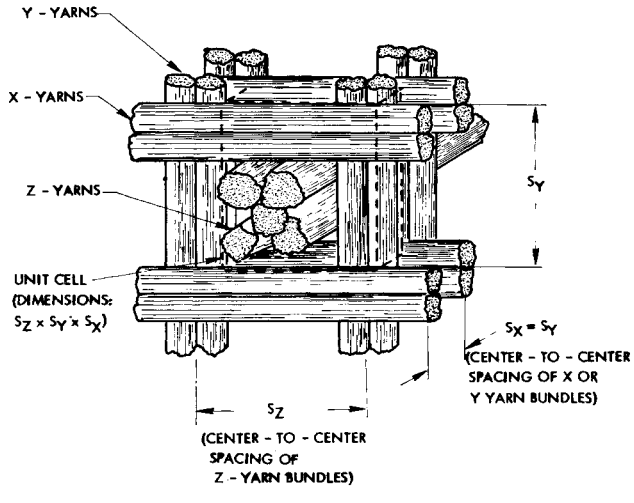

Fig. 1 3D preform geometrical parameters.

Received July 15, 1974; revision received December 9, 1974. This work was supported in part by the Re-Entry Vehicle Materials Technology (REVMAT) Program at the Naval Surface Weapons Center, White Oak, Silver Spring, Maryland under Contract N60921-74-C-0158 with Prototype Development Associates, Inc., Santa Ana, California. The support of the Naval Surface Weapons Center is greatly appreciated.

Index category: Structural Static Analysis.

* Assistant Professor, School of Engineering; Consultant, Prototype Development Associates, Santa Ana, Calif. Associate Member AIAA.

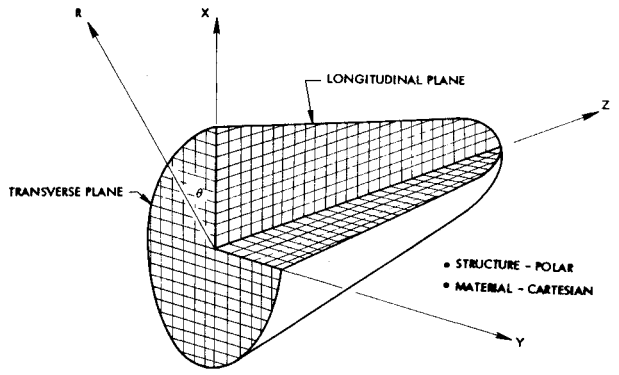

Fig. 2 Schematic relationship between structure coordinate system and material coordinate system.

in which the revised constitutive relations: a) account for the transverse orthotropy by including G_{xy} in the equations as an independent variable; b) degenerate to the transversely isotropic relations for $E_x = E_y = E$ and $G_{xy} = E_x/2(1+\nu_{xy})$; c) accurately predict the stresses for a rotating[5] and thermally loaded rectangularly orthotropic disk whereas analyses restricted to the assumption of transverse isotropy can have significant errors.

Revised Constitutive Relations

Elasticity Matrix

The usual technique in constructing an element stiffness matrix is to express the strain energy of the ith element in matrix quadratic form:

$$U_i = \tfrac{1}{2}\int_{v_i} \boldsymbol{\varepsilon}_i^T \boldsymbol{\sigma}_i \, dv_i = \tfrac{1}{2}\int_{v_i} \boldsymbol{\varepsilon}_i^T \mathbf{E}_i \boldsymbol{\varepsilon}_i \, dv_i = \tfrac{1}{2}\mathbf{D}_i^T \mathbf{K}_i \mathbf{D}_i \qquad (1)$$

where U_i = strain energy of ith element; v_i = volume of ith element; $\boldsymbol{\varepsilon}_i$ = vector of element strains (mxl); $\boldsymbol{\sigma}_i$ = vector of element stresses (mxl); $\mathbf{D}_i$ = vector of element nodal displacements (nxl); $\mathbf{E}_i$ = element elasticity matrix (mxm); $\mathbf{K}_i$ = element stiffness matrix (nxn).

For an axisymmetric solid-of-revolution the volume integral is usually expressed as

$$U_i = \tfrac{1}{2}\int_{v_i} \boldsymbol{\varepsilon}_i^T \mathbf{E}_i \boldsymbol{\varepsilon}_i \, dv_i = \tfrac{1}{2}\int_{A_i}\int_0^{2\pi} \boldsymbol{\varepsilon}_i^T \mathbf{E}_i \boldsymbol{\varepsilon}_i \, r \, d\theta \, dA_i = \tfrac{1}{2}2\pi \int_{A_i} \boldsymbol{\varepsilon}_i^T \mathbf{E}_i \boldsymbol{\varepsilon}_i \, r \, dA_i \qquad (2)$$

where the elasticity matrix $\mathbf{E}_i$ is independent of θ, i.e., no circumferential variation of material properties. However, since general orthotropic materials such as carbon-carbon can have engineering material properties which vary with direction between the principal material axes and therefore vary circumferentially, then a small modification of Eq. (2) is necessary to account for the variations.

Specifically,

$$U_i = \frac{1}{2}\int_{A_i}\int_0^{2\pi} \boldsymbol{\varepsilon}_i^T \mathbf{E}_i \boldsymbol{\varepsilon}_i \, r \, d\theta \, dA_i = \frac{1}{2}2\pi \int_{A_i} \boldsymbol{\varepsilon}_i^T \mathbf{E}_i^* \boldsymbol{\varepsilon}_i \, r \, dA_i \qquad (3)$$

where $\mathbf{E}_i^*$ is an elasticity matrix that accounts for the circumferential variation of properties. The revised elasticity matrix $\mathbf{E}_i^*$ is obtained by integrating each term of the elasticity matrix $\mathbf{E}_i$ with respect to the circumferential coordinate θ. A typical coefficient of $\mathbf{E}_i^*$ contains a combination of E_x, E_y, ν_{xy}, and G_{xy}.

Stress-Strain Transformations—xy-Plane

The modifications to the constitutive relations that reflect the material's transverse orthotropy are characterized by the stress-strain relations in the xy-plane. Thus to investigate the modifications to the element elasticity matrix $\mathbf{E}_i$, it is only necessary to focus on the stress-strain relations on the xy-plane.

The constitutive relations for stresses in the xy-plane can be expressed as

$$\begin{Bmatrix} \varepsilon_x \\ \varepsilon_y \\ \varepsilon_z \\ \gamma_{xy} \end{Bmatrix} = \begin{bmatrix} 1/E_x & -\nu_{xy}/E_x & -\nu_{xz}/E_x & 0 \\ -\nu_{xy}/E_x & 1/E_y & -\nu_{yz}/E_y & 0 \\ -\nu_{xz}/E_x & -\nu_{yz}/E_y & 1/E_z & 0 \\ 0 & 0 & 0 & 1/G_{xy} \end{bmatrix} \begin{Bmatrix} \sigma_x \\ \sigma_y \\ \sigma_z \\ \tau_{xy} \end{Bmatrix} \qquad (4)$$

or more compactly as

$$\boldsymbol{\varepsilon}_{xyz} = \mathbf{C}\boldsymbol{\sigma}_{xyz} \qquad (5)$$

The transformation of stresses from rectangular xyz to cylindrical coordinates shown schematically in Fig. 3, can be expressed by

$$\begin{Bmatrix} \sigma_r \\ \sigma_\theta \\ \sigma_z \\ \tau_{r\theta} \end{Bmatrix} = \begin{bmatrix} \cos^2\theta & \sin^2\theta & 0 & 2\sin\theta\cos\theta \\ \sin^2\theta & \cos^2\theta & 0 & -2\sin\theta\cos\theta \\ 0 & 0 & 1 & 0 \\ -\cos\theta\sin\theta & \cos\theta\sin\theta & 0 & \cos^2\theta - \sin^2\theta \end{bmatrix} \begin{Bmatrix} \sigma_x \\ \sigma_y \\ \sigma_z \\ \tau_{xy} \end{Bmatrix} \qquad (6)$$

or more compactly as

$$\boldsymbol{\sigma}_{r\theta z} = \mathbf{T}^{-1}\boldsymbol{\sigma}_{xyz} \qquad (7)$$

The transformation of strains from rectangular xyz to cylindrical $r\theta z$ coordinates can also be expressed compactly as

$$\boldsymbol{\varepsilon}_{r\theta z} = \mathbf{T}^T\boldsymbol{\varepsilon}_{xyz} \qquad (8)$$

where the transformation matrices $\mathbf{T}$ in Eqs. (7) and (8) are identical. By combining Eqs. (5, 7, and 8), the constitutive relations for the stresses in cylindrical coordinates can be expressed as

$$\boldsymbol{\varepsilon}_{r\theta z} = \mathbf{T}^T\mathbf{C}\mathbf{T}\boldsymbol{\sigma}_{r\theta z} = \mathbf{C}^*\boldsymbol{\sigma}_{r\theta z} \qquad (9)$$

where $\mathbf{C}^* = \mathbf{T}^T\mathbf{C}\mathbf{T}$. The coefficients of the 4×4 revised compliance matrix are displayed in Appendices A and B. The compliance matrix in Appendix A varies circumferentially and can be interpreted as being the inverse of the elasticity matrix $\mathbf{E}_i$ in Eq. (3). The compliance matrix in Appendix B, on the other hand, is the result of integrating each term of Appendix A with respect to the circumferential coordinate θ between $\theta = 0$ and $\theta = 2\pi$. The revised compliance matrix $\mathbf{C}^*$ in Appendix B—the inverse of the revised elasticity matrix $\mathbf{E}_i^*$ in Eq. (3)—can be thought of as a "weighted average" compliance matrix that accounts for the material property variations in the transverse plane. Although, in general, a symmetrically loaded rectangularly orthotropic solid-of-revolution is characterized by 3D asymmetric stresses and strains, the $\mathbf{C}^*$ matrix is an effort to account for material property variations while still retaining the computationally attractive axisymmetric 2D solution; hence the label, "weighted average."

A few points concerning the "weighted average" compliance matrix $\mathbf{C}^*$ are worth noting. First, solid-of-revolution computer

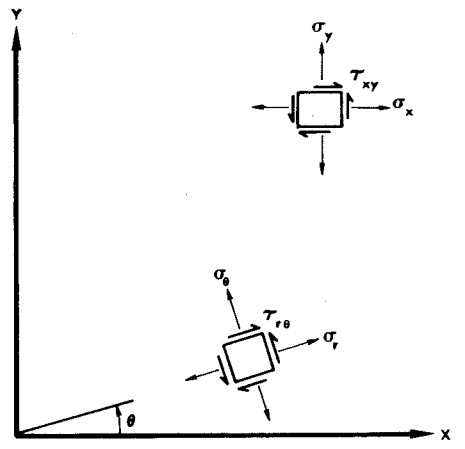

Fig. 3 Rectangular XYZ and polar $R\theta Z$ stress components in tranverse plane.

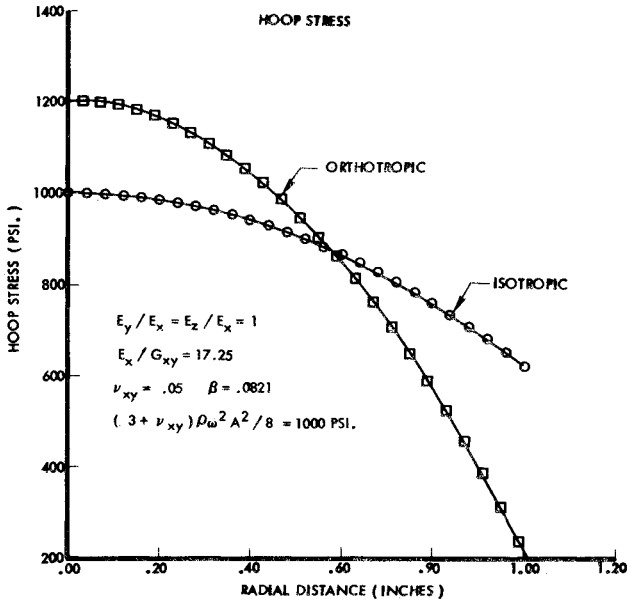

Fig. 4 Solid rotating orthotropic disk—hoop stress.

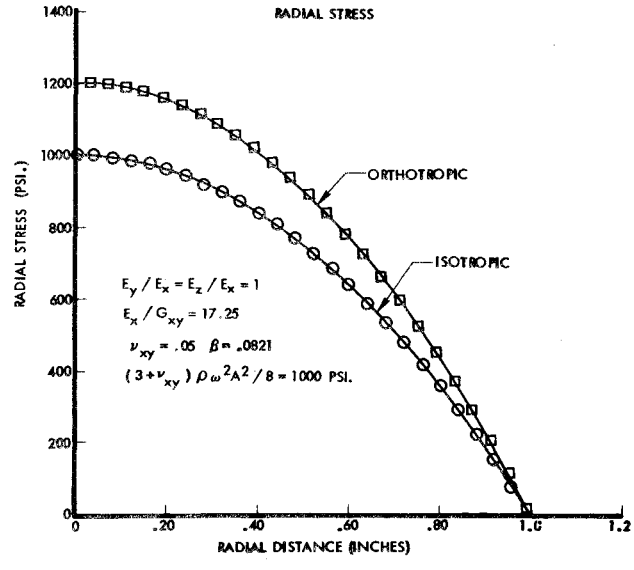

Fig. 5 Solid rotating orthotropic disk—radial stress.

codes such as SAAS III consider the stress components σ_r, σ_θ, σ_z, and τ_{rz} and assume stress components $\tau_{r\theta}$ and $\tau_{z\theta}$ are zero from symmetry conditions. Since $\mathbf{C}^*$ is related to the stress components σ_x, σ_y, σ_z, and τ_{xy}, the compliance coefficients related to the transverse shear stress τ_{xy} cannot be taken into account. In the proposed procedure the "weighted average" compliance matrix for a rectangularly orthotropic material is readily incorporated into SAAS III by replacing the $C_{44}{}^*$ term with $1/G_{xy}$. Secondly, a typical coefficient of $\mathbf{C}^*$ such as $C_{11}{}^*$ includes the transverse material properties such as E_x, E_y, ν_{xy} and G_{xy}. The effect of G_{xy} is particularly important since rectangularly orthotropic materials are usually characterized by a relatively low shear modulus. Note that for the degenerate case of $E_x = E_y$ and $G_{xy} = E_x/2(1+\nu_{xy})$ the $C_{11}{}^*$ coefficient becomes $1/E_x$ and the $C_{12}{}^*$ coefficient becomes $-\nu_{xy}/E_x$.

Results

Rotating Orthotropic Disk

To verify the accuracy of the revised constitutive relations, the stress distribution in a rotating, homogeneous, rectangularly orthotropic, thin disk was investigated. This classic example[5] provides a unique situation—the stress distribution is axisymmetric (function of radius only) even though the material is orthotropic. Thus the rotating disk problem serves as a check for the transversely orthotropic constitutive relations for a solid of revolution computer code such as SAAS III.

The polar coordinate stress components for the rotating disk can be expressed as (plane stress solution)

$$\sigma_r = \frac{\omega^2\rho a^2}{2}(1-\beta)\left(1-\frac{r^2}{a^2}\right)$$
$$\sigma_\theta = \frac{\omega^2\rho a^2}{2}\left\{(1-\beta)\left(1-\frac{r^2}{a^2}\right)+2\beta\frac{r^2}{a^2}\right\} \qquad (10)$$
$$\tau_{r\theta} = 0$$

where ω = angular velocity of the disk (rad/sec); ρ = mass density (mass/unit volume); a = outer radius of the disk; and r = radial coordinate. The anisotropy of the disk is characterized by the nondimensional parameter β defined as

$$\beta = \left[\frac{1}{E_x}+\frac{1}{E_y}-\frac{2\nu_{xy}}{E_x}\Big/\frac{3}{E_x}+\frac{3}{E_y}-\frac{2\nu_{xy}}{E_x}+\frac{1}{G_{xy}}\right] \qquad (11)$$

For the degenerate case of an isotropic disk with Poisson ratio ν, the anisotropy parameter β is $(1-\nu)/4$ which gives the stresses as

$$\sigma_R = (\omega^2\rho a^2/8)(3+\nu)(1-r^2/a^2)$$
$$\sigma_\theta = \frac{\omega^2\rho a^2}{8}(3+\nu)\left(1-\frac{1+3\nu}{3+\nu}\frac{r^2}{a^2}\right) \qquad (12)$$

which agrees, of course, with isotropic theory.

As an indication of how serious the errors in stress prediction can be when using the current constitutive relations, consider the plots of hoop and radial stress for the rotating anisotropic disk (Figs. 4 and 5). When the current constitutive relations are used, the hoop and radial stresses are identical to that of an isotropic rotating cylinder, i.e., the stresses do not in any way reflect the relatively low shear modulus ($E_x/G_{xy} = 17.25$). However, the modified constitutive relations do account for the transverse orthotropy and can be seen to agree with the theoretical results. Furthermore, it can be seen that the hoop and radial stresses are underestimated by about 16% at the center, while the hoop stress is overestimated by about a factor of 2 at the outer radius. The predicted hoop and radial stress values assuming other material property values ($E_z/E_x = 1$, $E_y/E_x = 10$, $E_x/G_{xy} = 17.25$) agreed equally as well with the theoretical results when using the revised constitutive relations.

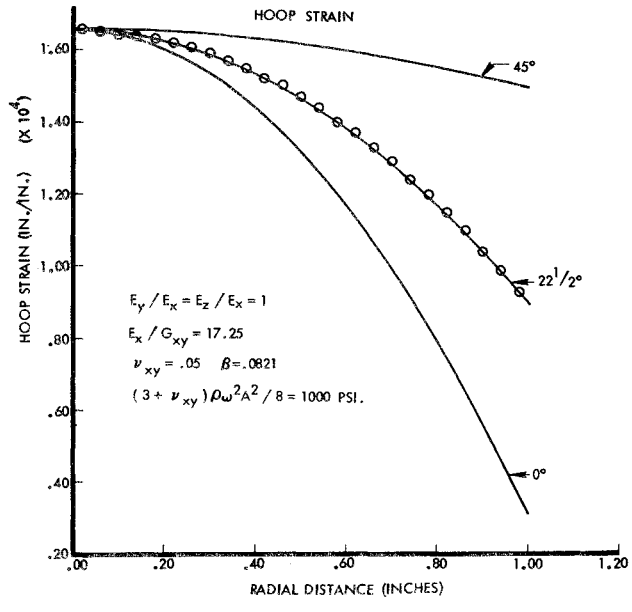

Fig. 6 Solid rotating orthotropic disk—hoop strain.

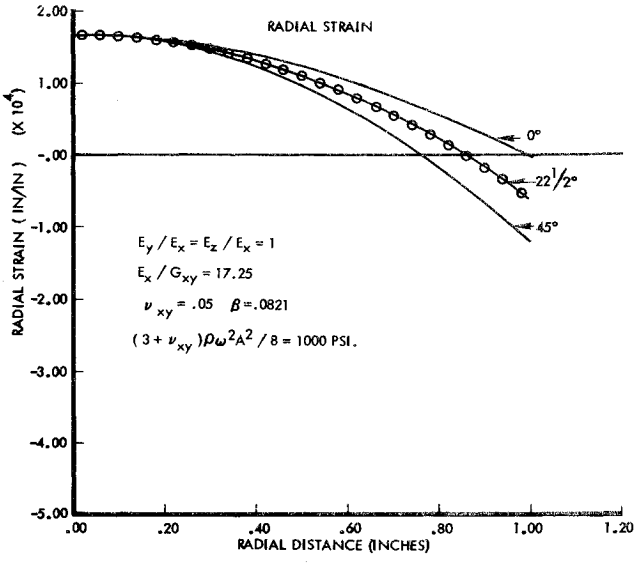

Fig. 7 Solid rotating orthotropic disk—radial strain.

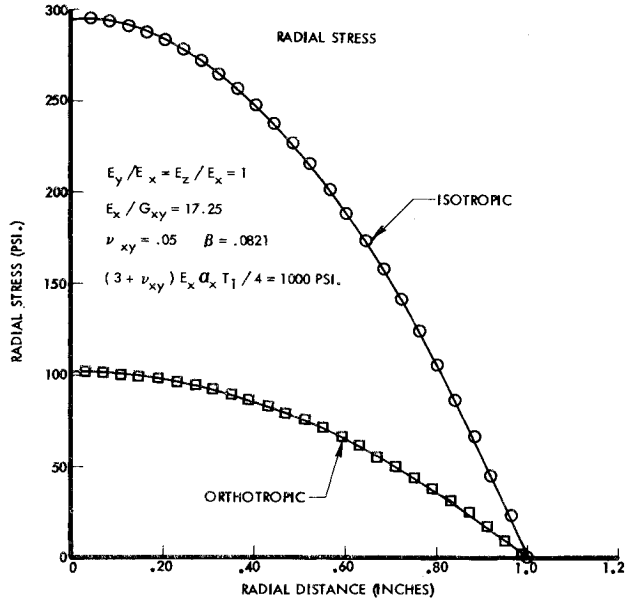

Fig. 9 Thermally loaded orthotropic disk—radial stress.

Whereas the hoop and radial stresses of a rotating orthotropic disk are axisymmetric, the strains do vary circumferentially. Inasmuch as the axisymmetric solid analysis provides such an excellent correlation for stresses when using the revised compliance matrix, it is of interest to compare the strains from the same analysis with the theoretical strains. To do so it is helpful to recognize that planes of symmetry for an axisymmetrically loaded composite material occur at multiples of $\pi/4$ from the composites' principal x-y directions when $E_x/E_y = 1$. Thus the hoop and radial strains within a 45° segment need only be investigated.

Figures 6 and 7 compare the theoretical hoop and radial strains at 0°, 22-1/2°, and 45° with those obtained from the SAAS III analysis. The figures support the notion of a "weighted average" compliance matrix—the strains obtained from the approximate analysis neither correspond to the maximum or minimum values which occur at 0° and 45°, but rather to the "average" theoretical values at 22½°.

Thermally Loaded Orthotropic Disk

Another application of particular interest is that of a thermally loaded disk. Composite materials such as carbon-carbon have found great favor among designers for critical re-entry vehicle components such as nosetips and heatshields. The fact that these components experience a severe thermal environment motivated the investigation of a circular disk subjected to a representative thermal gradient. Fortunately, an axisymmetric stress distribution for a rectangularly orthotropic disk can be achieved by choosing a temperature gradient of the form

$$T(r) = T_0 + T_1(r^2/a) \tag{13}$$

The solution to this thermal stress problem can be determined by superimposing the results of 3 separate loading conditions[6]—a hydrostatic pressure $E_x\alpha_x T_1(1-r^2/a^2)/(1-\nu_{xy})$, a surface tensile stress $E_x\alpha_x T_1/(1-\nu_{xy})$, and body force stresses derived from the body force potential $E_x\alpha_x T_1 r^2/a^2$. When these three load conditions are superimposed, the thermal stress components for a rectangularly orthotropic solid disk can be shown to be (plane stress solution)

$$\sigma_R = \beta\frac{E_x\alpha_x T_1}{(1-\nu_{xy})}\left(1-\frac{r^2}{a^2}\right)$$
$$\sigma_\theta = \beta\frac{E_x\alpha_x T_1}{(1-\nu_{xy})}\left(1-\frac{3r^2}{a^2}\right) \tag{14}$$

where it is assumed that the elastic moduli and coefficients of thermal expansion in the x and y directions are equal ($E_x/E_y = \alpha_x/\alpha_y = 1$). Again for the anisotropy parameter $\beta = (1-\nu)/4$, the previous results degenerate to those of isotropic theory

$$\sigma_R = (E_x\alpha_x T_1/4)(1-r^2/a^2)$$
$$\sigma_\theta = (E_x\alpha_x T_1/4)(1-3r^2/a^2) \tag{15}$$

Figures 8 and 9 depict how erroneous the thermal stress predictions can be for a composite material with a relatively low shear modulus ($E_x/G_{xy} = 17.25$). Whereas the SAAS III predictions, when using the revised compliance matrix, correspond to the theoretical results in Eq. (14), the predictions, when assuming transverse isotropy, correspond to the results in Eq. (15). For a material with a relatively low shear modulus the discrepancy in results can be quite significant. As an indication of how erroneous the stress predictions can be, consider the plot of nondimensional hoop and radial stresses vs the nondimensional shear modulus parameter E_x/G_{xy} shown in Fig. 10. Since the ratio of isotropic stress/orthotropic stress [compare Eqs. (14) and (15)] for both the hoop and radial stress are in the ratio $0.25\ (1-\nu_{xy})/\beta$, the ordinate values of Fig. 10 can be interpreted for either stress component. As can be seen from the graph, the ratio of isotropic to orthotropic thermal stresses increased significantly as E_x/G_{xy} increases; in

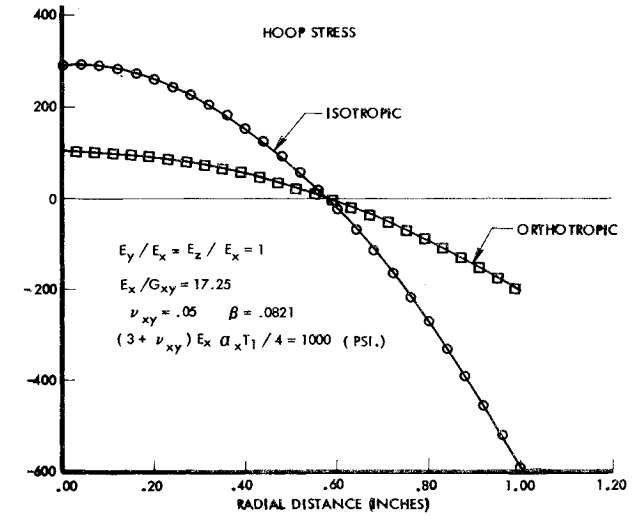

Fig. 8 Thermally loaded orthotropic disk—hoop stress.

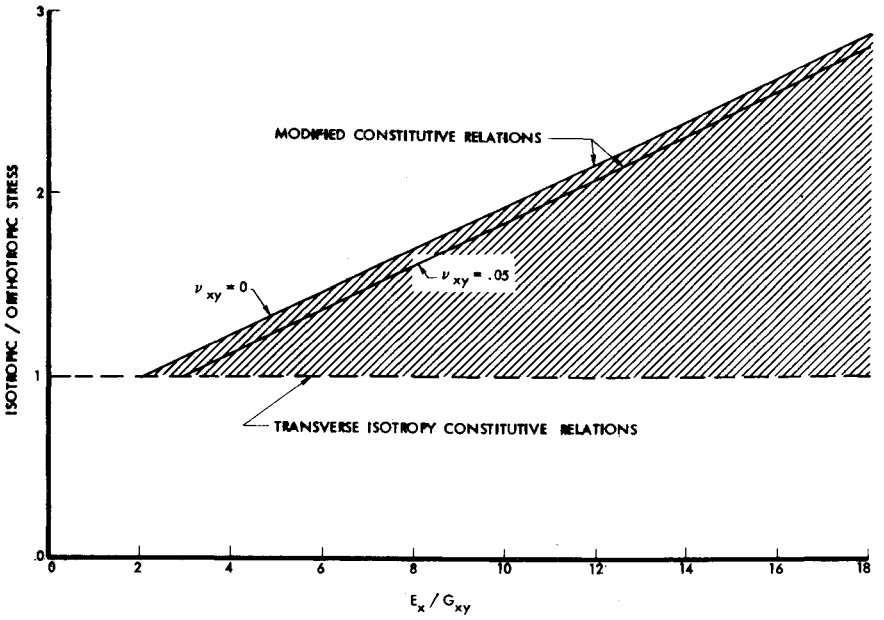

Fig. 10 Shear modulus effect on thermal stress predictions-isotropic vs orthotropic theory.

fact, for a realistic shear modulus parameter of $E_x/G_{xy} = 20$, the isotropic theory overpredicts the stresses by a factor of 3. The shaded region in Fig. 10 is a measure of the overprediction in stresses if the disk is assumed to be transversely isotropic.

As in the rotating disk analysis, the revised compliance matrix accurately predicts the axisymmetric thermal stress components. Again, it is of interest to correlate the SAAS III thermal strain predictions with the theoretical strain components at different angles of orientation. As in the rotating disk analysis, thermal strain predictions shown in Figs. 11 and 12 support the notion of the "weighted average" compliance matrix—the SAAS III predicted strains correspond to the "average" theoretical strains at $22\frac{1}{2}°$ rather than the maximum or minimum values which occur at 0° and 45°.

Strain Components

As suggested earlier in the discussion of the rotating disk and thermal stress problems, the predicted strains represent a "weighted average." However, since the modified compliance matrix (Appendix B) accurately predicts the axisymmetric stress components for body force, thermal and pressure loading on a solid disk, the strains in the principal material directions can be readily obtained by substituting the correct stress components into Eq. (4). In short, use the modified compliance matrix to predict the stresses and use Eq. (4) to predict the strains in the principal material directions.

Conclusions

A minor modification to the compliance matrix contained within the SAAS III or similar computer codes enables one to predict stresses for axisymmetrically loaded solid-of-revolution structures which are constructed from a rectangularly orthotropic material. Specifically the method has been shown to accurately predict the stresses in a rotating and thermally loaded rectangularly orthotropic solid disk. In some cases, the strains in the principal material directions can also be accurately predicted. The compliance matrix modifications account for the transverse orthotropy of a material by including the effect of G_{xy} in the equations. The modified compliance matrix also degenerates to the transversely isotropic form for $E_x = E_y$ and $G_{xy} = E_x/2(1+\nu_{xy})$.

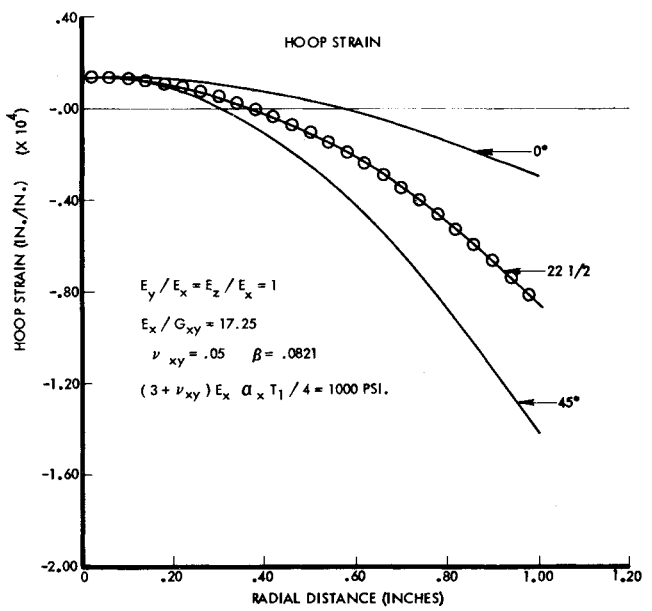

Fig. 11 Thermally loaded orthotropic disk—hoop strain.

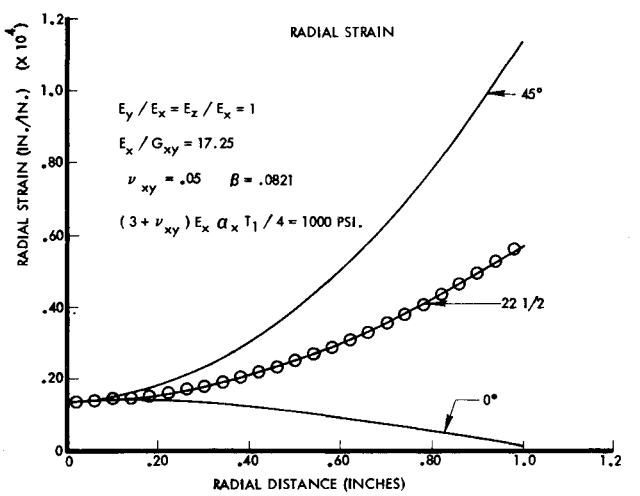

Fig. 12 Thermally loaded orthotropic disk—radial strain.

While it is recognized that an accurate and more general analysis can be performed with either a 3D[3] or pseudo 3D[4] code, these codes require considerably more computer time. Also the pseudo 3D approach requires additional modification.[7,8] The merit of the proposed technique is to provide an analyst with a computationally efficient, 2D analysis scheme for rectangularly orthotropic materials. It is suggested that the proposed 2D analysis can be used to identify an "optimum design" structure from several candidate designs before conducting the more costly 3D analysis on the "optimum design" candidate.

References

[1] Crose, J. G. and Jones, R. M., *SAAS III, Finite Element Stress Analysis of Axisymmetric and Plane Solids with Different Orthotropic, Temperature Dependent Material Properties in Tension and Compression,* TR-0059 (S6816-53)-1, June 1971, The Aerospace Corp., El Segundo, Calif.

[2] Hashin, Z., "Theory of Fiber Reinforced Materials," CR-1974, March 1972, NASA.

[3] Rashid, Y. R., "Three Dimensional Analysis of Elastic Solids—1 Analysis Procedure," *International Journal of Solids and Structures,* Vol. 5, 1969, pp. 1311–1331.

[4] Crose, J. G., *ASAAS, Asymmetric Stress Analysis of Axisymmetric Solids with Orthotropic Temperature Dependent Material Properties That Can Vary Circumferentially,* TR-0172 (S2816-15)-1, Dec. 1971, The Aerospace Corp., El Segundo, Calif.

[5] Lekhnitskii, S. G., *Anisotropic Plates,* Gordon and Breach, New York, 1968.

[6] Timoshenko, S. P. and Goodier, J. N., *Theory of Elasticity,* 2nd ed., McGraw-Hill, New York, 1951.

[7] Crose, J. G., private communication, Jan. 1974, Santa Ana, Calif.

[8] Geiler, D. E., "Thermostructural Analysis of Three-Dimensional Orthogonally Reinforced Carbon-Carbon Materials," *SAMPE Quarterly,* Vol. 19, April 1974, pp. 738–751.

Appendix A: Compliance Matrix

$$\mathbf{C}^* = \begin{bmatrix} \left\{\frac{C^4}{E_X}+\frac{S^4}{E_Y}-\frac{2C^2S^2\nu_{XY}}{E_X}+\frac{C^2S^2}{G_{XY}}\right\} & & & \text{Symmetric} \\ \left\{\frac{C^2S^2}{E_X}+\frac{C^2S^2}{E_Y}-\frac{C^4\nu_{XY}}{E_X}-\frac{S^4\nu_{XY}}{E_X}-\frac{C^2S^2}{G_{XY}}\right\} & \left\{\frac{S^4}{E_X}+\frac{C^4}{E_Y}-\frac{2C^2S^2\nu_{XY}}{E_X}+\frac{C^2S^2}{G_{XY}}\right\} & & \\ \left\{-\frac{C^2\nu_{XZ}}{E_X}-\frac{S^2\nu_{YZ}}{E_Y}\right\} & \left\{-\frac{S^2\nu_{XZ}}{E_X}-\frac{C^2\nu_{YZ}}{E_Y}\right\} & \frac{1}{E_Z} & \\ 2CS\left\{-\frac{C^2}{E_X}+\frac{S^2}{E_Y}+\frac{S^2\nu_{XY}}{E_X}-\frac{C^2\nu_{XY}}{E_X}+\frac{C^2-S^2}{2G_{XY}}\right\} & 2CS\left\{-\frac{S^2}{E_X}+\frac{C^2}{E_Y}-\frac{S^2\nu_{XY}}{E_X}+\frac{C^2\nu_{XY}}{E_X}-\frac{C^2-S^2}{2G_{XY}}\right\} & 2CS\left\{\frac{\nu_{XZ}}{E_X}-\frac{\nu_{YZ}}{E_Y}\right\} & \left\{4C^2S^2\left(\frac{1}{E_X}+\frac{1}{E_Y}+\frac{2\nu_{XY}}{E_X}\right)+\frac{(C^2-S^2)^2}{G_{XY}}\right\} \end{bmatrix}$$

where $C = \cos\theta$ and $S = \sin\theta$.

Appendix B: Compliance Matrix

$$\mathbf{C}^* = 2\pi\begin{bmatrix} \left\{\frac{3}{8}\left(\frac{1}{E_X}+\frac{1}{E_Y}\right)-\frac{\nu_{XY}}{4E_X}+\frac{1}{8G_{XY}}\right\} & & & \text{Symmetric} \\ \left\{\frac{1}{8}\left(\frac{1}{E_X}+\frac{1}{E_Y}\right)-\frac{3\nu_{XY}}{4E_X}-\frac{1}{8G_{XY}}\right\} & \left\{\frac{3}{8}\left(\frac{1}{E_X}+\frac{1}{E_Y}\right)-\frac{\nu_{XY}}{4E_X}+\frac{1}{8G_{XY}}\right\} & & \\ \left\{-\frac{\nu_{XZ}}{2E_X}-\frac{\nu_{YZ}}{2E_Y}\right\} & \left\{-\frac{\nu_{XZ}}{2E_X}-\frac{\nu_{YZ}}{2E_Y}\right\} & \frac{1}{E_Z} & \\ 0 & 0 & 0 & \left\{\frac{1}{2}\left(\frac{1}{E_X}+\frac{1}{E_Y}+\frac{2\nu_{XY}}{E_X}\right)+\frac{1}{2G_{XY}}\right\} \end{bmatrix}$$